Proceedings of ICAPP '12
Chicago, USA, June 24-28, 2012
Paper 12xxx

Benchmarking of Software and Methods for Use in Transient Multidimensional Fuel Performance with Spatial Reactor Kinetics*

J. E. Banfield,[1] K. T Clarno,[2] S. P. Hamilton,[2] G. I. Maldonado,[1] B. Philip,[2] and M. L. Baird[2]

[1]*Department of Nuclear Engineering, University of Tennessee*
Knoxville, TN 37996-2300
Tel: 662-832-2143, Fax: 865-574-3527, Email: banfieldje@ornl.gov

[2]*Oak Ridge National Laboratory*
Oak Ridge, TN 37831

Abstract – *The key physics involved in accurate prediction of reactor-fuel-element behavior includes neutron transport and thermal hydraulics. The thermal hydraulic feedback mechanism is primarily provided through cross sections to the neutron transport that are temperature and density dependent. Historically, this coupling was primarily seen only in reactor simulators, which are well suited to model the reactor core, giving only a coarse treatment to individual fuel pins as well as simple models for thermal distribution calculations. This poor resolution on the primary coupling mechanisms can lead to conservatisms that should be removed to improve fuel design and performance. This work seeks to address the resolution of space-time-dependent neutron kinetics with thermal feedback within the fuel pin scale in the multiphysics framework. The specific application of this new capability is transient performance analysis of space-time-dependent temperature distribution of fuel elements. The coupling between the neutron transport and the thermal feedback is extremely important in this highly coupled problem, primarily applicable to reactivity-initiated-accidents (RIAs) and loss-of-coolant-accidents (LOCAs). The capability developed will include the coupling of the time-dependent neutron transport with the time-dependent thermal diffusion capability. An improvement in resolution and coupling is proposed by developing neutron transport models that are internally coupled with high fidelity within fuel pin thermal calculations in a multiphysics framework. Good agreement is shown with benchmarks and problems from the literature of RIAs and LOCAs for the tools used.*

I. INTRODUCTION

The key physics involved in accurate prediction of reactor-fuel-element behavior includes neutron transport and thermal hydraulics. The thermal hydraulic feedback mechanism is primarily provided through cross sections to the neutron transport that are temperature and density dependent. To develop these models, accurate models are needed for multidimensional eigenvalue calculations, spatial kinetics, and the feedback mechanism provided by thermal hydraulics. To facilitate this coupling, a series of semi-coupled models has been evaluated to develop a foundation for the spatial kinetics with intra-pin powers and thermal feedback. These models include point kinetics with and without feedback, spatial kinetics without feedback, and multidimensional transport mapped to multidimensional thermal solutions.

To model this highly coupled multiphysics problem, several existing simulation tools were leveraged. The multiphysics framework for this effort

*Notice: This manuscript has been authored by UT-Battelle, LLC, under contract DE-AC05-00OR22725 with the U.S. Department of Energy. The United States Government retains and the publisher, by accepting the article for publication, acknowledges that the United States Government retains a non-exclusive, paid-up, irrevocable, world-wide license to publish or reproduce the published form of this manuscript, or allow others to do so, for United States Government purposes.

is the Advanced Multi-Physics (AMP)[1] Integrated Performance and Safety Code. The AMP code provides the nuclear-fuel-performance transient thermal calculation in addition to the aforementioned multiphysics framework. The neutronics analysis will be provided by the Denovo[2] radiation transport code, which is internally coupled with AMP. The point-kinetics equations are solved with the neutron-kinetics component from the Burner Reactor Integrated Safety Code (BRISC),[3] which has also been coupled within AMP. The temperature-dependent cross sections were prepared with the SCALE[2] code, using the CSAS-I and TRITON modules.

AMP and Denovo have been benchmarked for their respective physics; [1,4] the kinetics module from BRISC (KMB), however, did not include published results. Therefore, this report also contains an independent verification of KMB. In addition, this paper presents a modified quasi-static kinetics implementation with corresponding verification of Denovo.

The problem of interest for these tools is a control rod ejection study. This study will be done on a mini-assembly, which will consist of a 3 × 3 array of fuel pins with a control rod in the center. Considering that the scale of typical core simulator calculations is pin-resolved powers while this study will focus on within-pin-resolved powers, this scaling is consistent with the 3 × 3 mini-core used in Hursin and Downar [5]. Furthermore, Hursin and Downar[5] demonstrate the general trends expected for power excursion from a reactivity-initiated-accident (RIA) from a control rod ejection with and without thermal feedback, thereby demonstrating the impact of incorporating thermal feedback. As temperature differences within a fuel pin can be upwards of a thousand Kelvin and fuel performance codes that calculate thermal response are extremely sensitive to power inputs,[6] this resolution should help to expose under- and overconservatisms in the current methods. This new resolution of intra-pin is evident from a review of current methods, as shown in Hursin and Downar[5] and Diamond, Bromley, and Aronson.[7]

II. METHODOLOGY

II.A. Point Kinetics

The following equations represent the point-kinetics ordinary differential equations (ODEs). Equation (1) represents the rate of change of the six precursor concentrations as functions of time. In this equation, C is the precursor concentration, t is time, β is the delayed neutron fraction, $P(t)$ is the power, and λ is the decay constant. Equation (2) represents the rate of change of the power as a function of time, where ρ is the reactivity insertion as a function of time, and Λ is the mean generation time.

$$\frac{dC_i(t)}{dt} = \frac{\beta_i}{\Lambda} P(t) - \lambda_i C_i(t), i = 1,...,6 \qquad (1)$$

$$\frac{dP(t)}{dt} = \frac{\rho(t) - \beta}{\Lambda} P(t) + \sum_{i=1}^{6} \lambda_i C_i(t) \qquad (2)$$

Including thermal feedback adds one additional ODE to the system, which is shown in Eq. (3).[8] In this equation, T is temperature, c_p is specific heat capacity, ε is the fraction of fission energy deposited as heat, H is height, D is diameter, A is a material-dependent constant, T_c is coolant temperature, and t is time (where the geometry considered is a cylinder).

$$\frac{dT(t)}{dt} = \frac{1}{c_p}[\varepsilon P(t) - \frac{AHD^{0.75}[T(t) - T_c]^{1.25}}{T(t)^{0.25}}] \qquad (3)$$

II.B. Quasi-Static Spatial Kinetics

In the quasi-static kinetics implmentation, the time-dependent angular flux is assumed to be the product of weakly time-dependent angular flux multiplied by an amplitude function, which is only a function of time. This pseudo separation of variables is shown in Eq. (4), where ψ is the true time-dependent angular flux, Ψ is the weakly time-dependent angular flux and T is the amplitude function. The Boltzmann neutron transport equation with explicit representation of delayed neutrons can be written as shown in Eq. (5). In this implementation, the time-dependent rate of change of angular flux with respect to time has been neglected. This is a first approximation based on the fact that for the fast reactor modeled, the inverse velocity is quite low, which makes this term a higher-order factor. This approach was taken because of a current inability in Denovo to save angular fluxes from one run to the next.

$$\psi(r, E, \Omega, t) = \Psi(r, E, \Omega, t) T(t) \qquad (4)$$

$$\begin{aligned}
&\Omega\nabla\Psi(r,E,\Omega,t)+\Sigma_t(r,E,t)\Psi(r,E,\Omega,t)\\
&-\iint\Sigma_s(r,E'\to E,\Omega'\to\Omega,t)\\
&\bullet\Psi(r,E',\Omega',t)dE'd\Omega'\\
&-\chi_p(r,E)(1-\beta)\iint\upsilon(r,E')\Sigma_f(r,E',t)\\
&\bullet\Psi(r,E',\Omega',t)dE'd\Omega'\\
&=\frac{1}{T(t)}\sum_i\lambda_i C_i(r,t)\chi_i(r,E)
\end{aligned}\tag{5}$$

In Eq. (5), Ω represents the normal vector in each direction for each angle, Ψ represents angular flux, Σ_t represents a macroscopic total cross section, Σ_s represents a macroscopic scattering cross section, χ_p represents prompt fission yield, β represents total delayed neutron fraction, v represents neutrons per fission, Σ_f represents a macroscopic fission cross section, T represents power at time t (obtained from the point-kinetics equations), λ represents a decay constant, C represents a precursor concentration, i represents a precursor group, and χ_i represents a precursor neutron yield. The rate of change of precursors is given in Eq. (6).

$$\begin{aligned}
&\frac{\partial}{\partial t}C_i(r,t)=\iint\upsilon(r,E')\beta_i\Sigma_f(r,E',t)\\
&\bullet\Psi(r,E',\Omega',t)dE'd\Omega'-\lambda_i C_i(r,t)
\end{aligned}\tag{6}$$

If the approximation is made such that the precursor concentrations are decoupled from each other through a time-average representation of the flux (or alternatively the power, similar to the point-kinetics formulations), Eq. (6) can be solved in an analytical fashion to yield Eq. (7), which is the time-dependent concentration of precursor isotopes.

$$C_i(r,t)=C_o(r,t)e^{(-\lambda t)}+\frac{1}{\lambda}T(\bar{t})P(\bar{t})\beta_i\chi_i(1-e^{-\lambda t})\tag{7}$$

In this equation, P is the power. This is the formulation that has been implemented using Denovo through a simplified implementation of the improved quasi-static method.[9]

III. RESULTS

To develop the spatial kinetics with spatial thermal feedback capability, a comparison for the expected trend in power was needed. As has been established in numerous references, including Hursin and Downar[5] and Diamond, Bromley, and Aronson,[7] the primary mechanism of thermal feedback for spatial kinetics comes through cross sections. To simulate this effect for point kinetics, also developed in Goluoglu and Dodds,[9] as well as make a comparison to the new spatial thermal feedback (for point kinetics) capabilities implemented within the AMP framework, reactivity coefficients are calculated from transport solutions. For this work these coefficients were primarily obtained with the NEWT code.

III.A. Point Kinetics without Thermal Feedback for Amplitude Calculation

If thermal feedback is neglected, the point-kinetics equations predict an exponential jump in power followed by a slow exponential rise in power. The KMB code implemented within AMP is compared to an externally developed Runge-Kutta multistep predictor-corrector fourth- and fifth-order (RK45) code for comparison purposes. In addition, both codes are compared to a one-group formulation for the same problem, which can be solved analytically. Figure 1 and Table I depict the verification of the point-kinetics package KMB implemented within AMP. Both solutions were shown as convergent under mesh refinement with comparable run times of less than 1 min with a time step of .01 s for the problem shown.

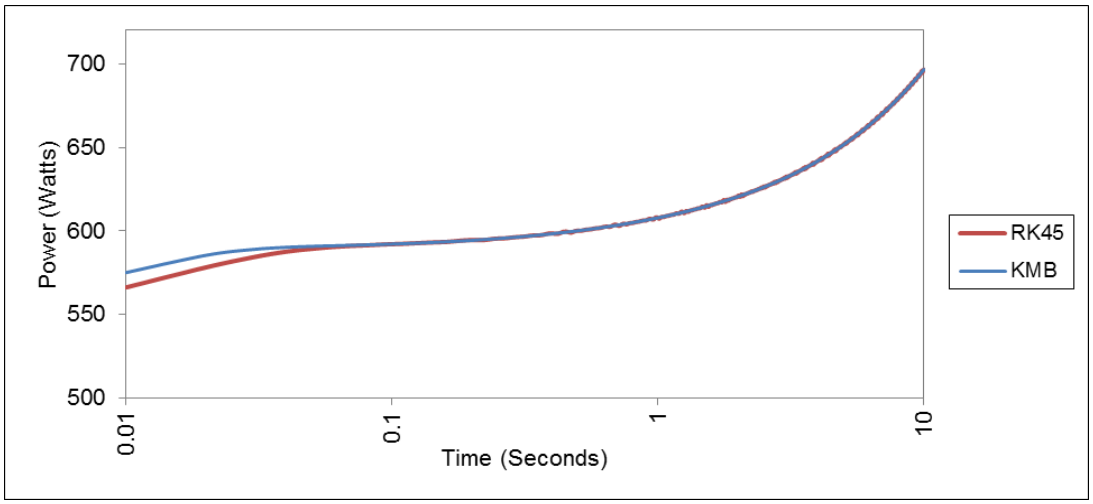

Fig. 1. KMB vs. RK45.

TABLE I

BRISC vs. RK45 vs. AMP Comparison**

** - 3 s Transient, Fixed Reactivity Insertion, Starting Po = 543 W Δt=.01 s

Quantity	Power (W)	Power Change (W)	Power Percent Error (from RK45)	Power Percent Error (from Analytic)
Six-group (BRISC)	**631.277**	88.277	-0.01%	1.72%
Six-group (RK45)	**631.206**	88.206		1.71%
One-group (Analytic)	**620.6**	77.6	1.68%	
Six-group (AMP)	**631.295**	88.295	-0.01%	1.72%

III.B. Point Kinetics with Thermal Feedback for Loss-of-Coolant-Accidents Analysis

For comparison the point-kinetics parameters developed in Dodds and Westfall[8] for use with the point-kinetics-with-feedback model were used. The problem considered was a step change in reactivity using six neutron precursor groups and thermal feedback through a reactivity coefficient expressed in cents per degrees Celsius. The problem was run over 1000 min, simulating an extended transient (more than 10 h). The code developed for this work used a Runge-Kutta multistep predictor corrector method using off-the-shelf academic computational tools. This code is compared to SKINATH, developed in Dodds and Westfall.[8]

This method is similar to the methodology employed in AMP. However, the temperature distribution is calculated by a 3D transient thermal solver within AMP using the IDA[10] time integrator. This integrator drives both the thermal and power calculations in AMP.

The power and temperatures as a function of time from the reference SKINATH and the RK45 code developed are shown in Figs. 2 and 3. The RK45 time integrator was a higher-order method relative to the first-order method (LSODE) used by SKINATH. This is probably the reason the peak power predicted by the RK45 method is larger than that predicted by SKINATH. As the peak power occurs slightly later in the RK45 method, the SKINATH power oscillations lead the RK45 oscillations throughout the rest of the transient. This

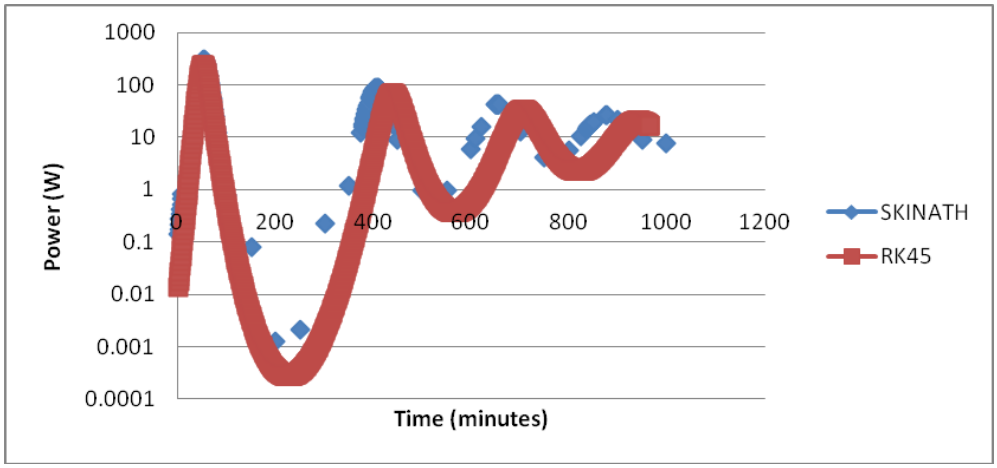

Fig. 2. Power comparison (RK45 vs. SKINATH[8]).

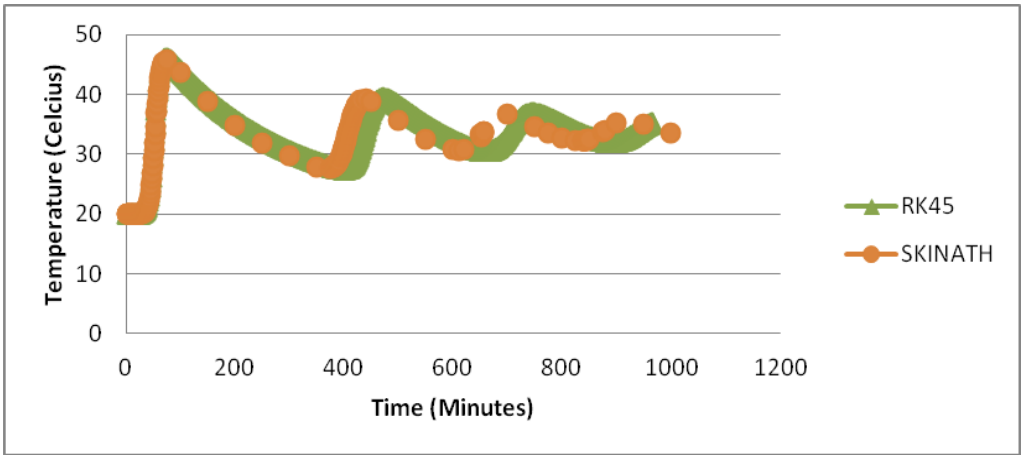

Fig. 3. Temperature comparison (RK45 vs. SKINATH[8]).

agreement and the trends are consisent with the agreement demonstrated in Dodds and Westfall[8] against an RK4 method. Similar trends and results are seen in the temperature figure (Fig. 3).

III.C. Spatial Kinetics without Feedback for RIA Analysis

To verify the kinetics implementation, the transport implementation must be correct because the transport provides the powers (or fluxes) for the kinetics calculations. The benchmark selected for this effort was Argonne National Laboratory (ANL) benchmark problem 16-A1, which is a 1D spatial-kinetics benchmark for a sodium fast reactor.[11] The problem features seven material regions of fuel blankets, fuel regions, sodium regions, and two energy groups, whose cross sections are provided in the benchmark. The first step in the spatial-kinetics process is the eigenvalue calculation. A problem was run with reflecting boundary conditions on the top and bottom to convert the problem to 1D. The eigenvalue was within 1 pcm of the 1.000198 reported in the benchmark. The spatial-flux comparison is shown in Fig. 4. All of the fluxes were within 1% of the benchmark.

To continue the development of the spatial-kinetics capability for AMP, the next step was to obtain the perturbed flux neglecting the time-dependent flux term. This was done as a starting point, as the Denovo transport code does not currently contain a way to save angular fluxes, which are needed for the subsequent step if the time-dependent flux term is to be used. Neglecting this

term simplifies the pseudo separation of variables used in the quasi-static method, as the amplitude function (T(t)) is present in every term. Thus, dividing by this term removes the amplitude function from the shape equation. The initial fluxes come from the eigenvalue solution shown in Fig. 4. The perturbation is a change in material densities in the leftmost fissile regions, which constitutes an increase in the fission cross sections, as well as a decrease in the material density in the rightmost fuel region. The second flux solution, the perturbed solution, is run as a fixed-source problem. This problem is run using steady-state spatially dependent precursors as the fixed source. The comparison of the perturbed steady-state fluxes to the flux at some short time (t = .01 s) after the perturbation is shown in Fig. 5. The fluxes from the kinetics method used with the Denovo code at t = .01 s were within 5% of the fluxes given in the 16-A1 benchmark. These differences are primarily attributable to neglecting of the time-dependent angular flux change term in the kinetics equations.

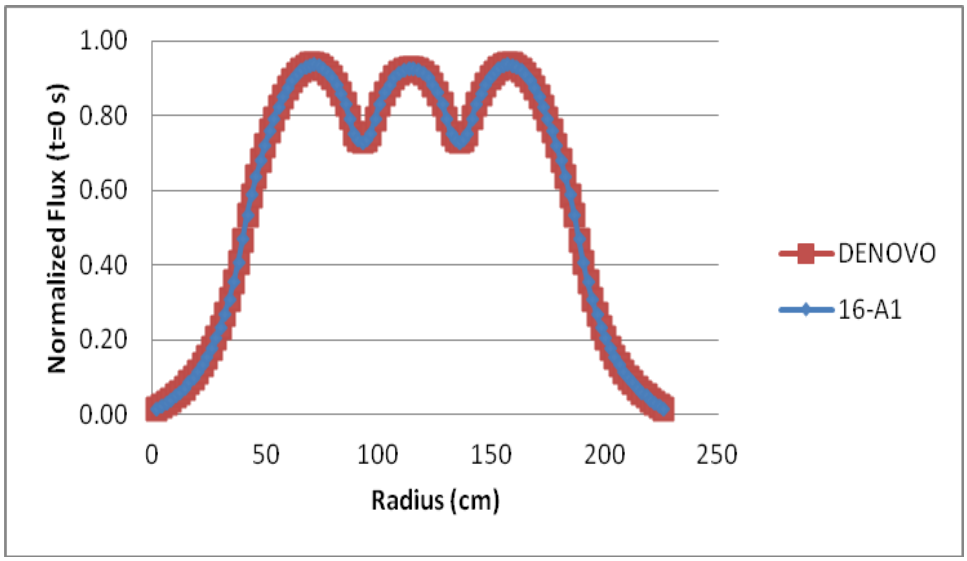

Fig. 4. Denovo vs. 16-A1 benchmark flux solution (Group 1).

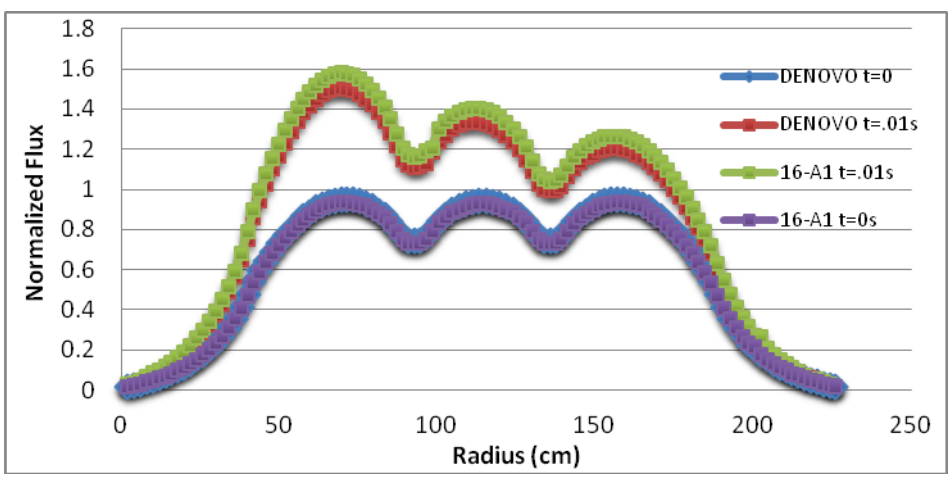

Fig. 5. Denovo vs. 16-A1 perturbed flux (Group 1).

The next calculation required for quasi-static kinetics is the amplitude function, which is only a function of time. It will become important when the time-dependent term is included. To calculate the amplitude function, point kinetics is used. The parameters for the point kinetics solutions should come from the adjoint flux collapsed over energy and angle. As the adjoint has not yet been calculated for

this problem, for these preliminary proof-of-principle studies, the point-kinetics parameters presented in Goluoglu and Dodds[9] were used. The comparison of the amplitude function using RK45, Padé order three rational approximant (AMP), and 16-A1 benchmark, as well as the powers from the spatial-kinetics calculations, are shown in Fig. 6. The magnitudes of the power from the kinetics method with the Denovo code at t = .01s and the power from the 16-A1 benchmark were within 3%. This difference is again attributable to neglecting of the time-dependent rate of angular flux in the kinetics method used with the Denovo code. The powers from the point-kinetics methods were within 2% of the powers from the benchmark. These differences are probably attributable to slightly different reactivity insertions used in the early time steps, as well as time step differences. AMP and KMB use uniform .01 s steps, which were shown as convergent under mesh refinement; therefore, a constant reactivity insertion was used for the first .01 s in AMP and KMB. This was not the case in the benchmark. Denovo similarly was used with a constant reactivity insertion, accounting for the overpredicted powers at less than .01 s.

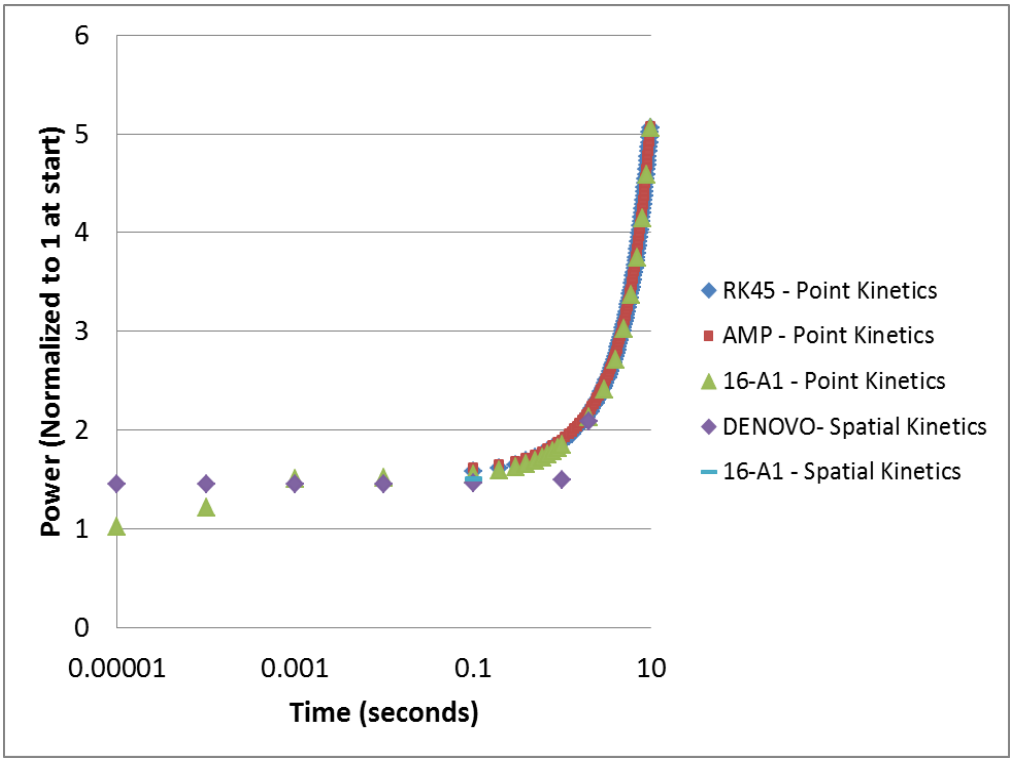

Fig. 6. RK45 vs. AMP and 16-A1 amplitude.

III.D. Eigenvalue Solutions for Initial Power Profiles of Spatial Kinetics with Thermal Feedback

The first step in obtaining the space/time-dependent power and temperature distributions is to calculate the steady-state power profiles. Denovo was used within AMP to calculate the eigenvalue solution. These powers were mapped into AMP to calculate the corresponding steady-state thermal solution for each pin, which was decoupled in AMP. This steady state will be the initial condition for control rod ejection.

The results of the Denovo and corresponding NEWT solution are shown in Fig. 7.

The geometry for the control rod ejection problem is a 3 × 3 mini-assembly. This geometry was modeled in NEWT. NEWT, within SCALE, employs a rigorous cross-section treatment able to provide multigroup cross sections that preserve reaction rates from 1D continuous energy data (from CENTRM) through the 238-group ENDF library. The CSAS-I module within SCALE was also used to generate cross sections for Denovo. The NEWT results were compared with the Denovo results, and the eigenvalues were 145 pcm different. Denovo yielded a k_{eff} of 1.06899, while NEWT yielded a k_{eff} of 1.07054. These differences are attributable to the

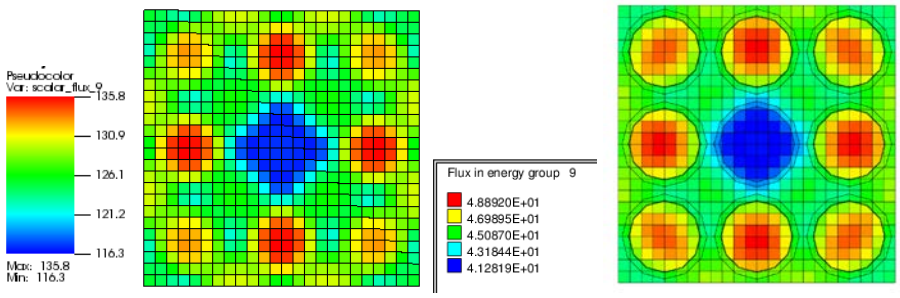

Fig. 7. Denovo multipin solution unnormalized fast flux (left) and NEWT unnormalized fast flux (right).

unstructured mesh used in NEWT versus the structured mesh used in Denovo, as is evident in Fig. 7. Further spatial and angular mesh refinement is expected to lower these differences.

The transient thermal calculation piece of AMP has been verified in Lebrun-Grandie and Patel[12]. AMP now has the capability to map a multipin transport solution to a corresponding thermal calculation. For this work the initial capablity developed included mapping an intrapellet power distribution to a transient thermal calculation using the IDA time integrator. The process being developed will be run in the following manner. First, the fixed-source iterations for the kinetics will be calculated by the Denovo code within AMP. Then this power will be mapped to the AMP transient thermal calculation. Finally, the transient thermal calculation will pass back the intrapin temperature distribution after some time, which will be used to update the temperature-dependent cross sections for the next fixed-source kinetics calculation.

IV. CONCLUSION

We have developed a methodology for implementing space-time-dependent coupled power-temperature distributions within a multiphysics framework. This development includes the steady-state and transient development and benchmarking of the Denovo transport code with regards to the ANL 16-A1 benchmark. In a coordinated development, external verification codes as well as point-kinetics codes were written and internally coupled within AMP for the calculation of point kinetics with and without thermal feedback for loss-of-coolant accident analysis, which was also developed within the multiphysics framework. These analyses were verified through comparisons with analytic solutions and code-to-code verifications. A method for mapping from the Denovo transport code to the AMP nuclear fuel performance code was developed for calculation of steady-state and transient thermal distributions with interaction and feedback with the point-kinetics code implemented within AMP. For the next phase of development, the SCALE code was used to develop temperature-dependent cross sections for use in coupled RIA analysis with intrapin power and temperature distributions with feedback, which was benchmarked against the AMP-Denovo steady-state-calculated intial conditions for the RIA transient.

REFERENCES

1. J. E. BANFIELD et al., *The AMP (Advanced MultiPhysics) Nuclear Fuel Integrated Performance and Safety Code*, ORNL/LTR-2011/42, Technical Memo, Oak Ridge National Laboratory, Oak Ridge, TN (2011).

2. *SCALE: A Comprehensive Modeling and Simulation Suite for Nuclear Safety Analysis and Design*, ORNL/TM-2005/39, Version 6.1, Oak Ridge National Laboratory, Oak Ridge, TN (2011). Available from Radiation Safety Information Computational Center at Oak Ridge National Laboratory as CCC-785.

3. R. C. SCHMIDT et al., *Foundational Development of an Advanced Nuclear Reactor Integrated Safety Code Sandia Report*, SAND2010-0878, Sandia National Laboratories, Albuquerque, NM (2010).

4. T. M. EVANS et al., "Denovo – A new three-dimensional parallel discrete ordinates code in SCALE," *Nucl. Technol.*, **171**, 171–200 (2010).

5. M. HURSIN and T. Downar, "PWR Control Rod Ejection Analysis with the MOC Code DECART," Joint International Workshop:

Nuclear Technology Society–Needs for Next Generation, Berkley, CA, January 6–8, 2008.

6. "Mixed-oxide (MOX) Fuel Performance Benchmark," compiled by Terje Tverberg, NEA/NSC/DOC(2007)6, Nuclear Energy Agency, Organisation for Economic Co-Operation and Development (2007).

7. D. J. DIAMOND, B. P. Bromley, and A. L. ARONSON, *Power Level Effect in a PWR Rod Ejection Accident*, BNL-NUREG-69285, Brookhaven National Laboratory, Brookhaven, NY (2002).

8. H. L. DODDS, and R. M. Westfall, *SKINATH–A Computer Program for Solving the Reactor Point Kinetics Equations with Simple Thermal-Hydraulic Feedback*, ORNL/CSD/TM-210, Oak Ridge National Laboratory, Oak Ridge, TN (1984).

9. S. GOLUOGLU and H. L. Dodds, "A Time-Dependent, Three-Dimensional Neutron Transport Methodology," *Nucl. Sci. Eng.*, **139**, 248–261 (2001).

10. A. C. HINDMARSH, R. Serban, and A. Collier, "User Documentation for IDA v2.60," UCRL-SM-208112, Lawrence Livermore National Laboratory, Livermore, CA (2009).

11. Mathematics and Computation Division of the American Nuclear Society, *National Energy Software Center: Benchmark Problem Book*, Supplement 3, ANL-7416, Argonne National Laboratory, Argonne, IL (1986).

12. D. LEBRUN-GRANDIE and S. Patel, "Verification of the AMP (Advanced Multi-Physics) Nuclear Fuel Performance Code," ORNL Poster, Oak Ridge National Laboratory, Oak Ridge, TN (2011).